Two-phase equilibria and nucleation barriers near a critical point

H. Furukawa* and K. Binder
Institut für Festkörperforschung, Kernforschungsanlage Jülich, D-5170 Jülich, Postfach 1913, West Germany
(Received 12 November 1981)

A liquid-gas system at temperatures below criticality and densities between the liquid and the gas density at the coexistence curve exhibits equilibrium between a spherical liquid domain and the surrounding gas. This two-phase state is studied for the three-dimensional lattice-gas model, with the use of Monte Carlo methods. In sampling the chemical potential of lattices which are finite but much larger than the correlation length for various densities, the radius R of the liquid cluster is derived from the excess density without any ambiguities in the cluster definition. From the relation between cluster radius and excess chemical potential, information on the *universal* scaled interface free energy of clusters as a function of R/ξ is obtained, in the range $3 \lesssim R/\xi \lesssim 10$, which is also the range of experimental interest. The resulting free-energy barriers against nucleation deviate distinctly from the capillarity approximation in most parts of this regime. At temperatures far below criticality, the present method is shown to agree with the standard approach where a cluster is defined in terms of the contour around occupied lattice sites. Finally, the consequences of our results for experiments and phenomenological droplet models are briefly discussed.

I. INTRODUCTION

A theoretical understanding of the free energy of formation of the microscopic nucleus of the new phase at a first-order phase transition has been a longstanding problem in statistical mechanics.[1-4] The standard approach ("classical theory") assumes nuclei ("droplets") of spherical shape and decomposes their formation free energy ΔF into a bulk term proportional to the volume of the droplet, and a surface term where one uses the interface tension f_I appropriate for a flat interface between macroscopic bulk phases. For three-dimensional liquid-gas systems (Fig. 1), the bulk term is hence $(4\pi R^3/3)\delta\mu\Delta\rho$, where $\delta\mu=\mu-\mu_{\text{coex}}$, the chemical potential difference between the considered (metastable) state and the state at the coexistence curve $\Delta\rho=\rho_{\text{liquid}}-\rho_{\text{gas}}$. Thus,

$$\Delta F_{\text{class}} = -(4\pi R^3/3)\delta\mu\Delta\rho + 4\pi R^2 f_I \ . \qquad (1)$$

While it is commonly accepted that Eq. (1) becomes asymptotically valid in the limit $R\to\infty$, one has to expect correction terms to Eq. (1) for the finite values of R which are of physical interest, i.e., $5\xi \lesssim R \lesssim 10\xi$, where ξ is the correlation length of density fluctuations [the "intrinsic" thickness of the liquid-gas interface is of the same order of magnitude as ξ, (see Ref. 15)]. For smaller R/ξ the decomposition of the droplet formation energy in bulk and surface terms is even expected to break down; though phenomenological assumptions for ΔF in this regime have also been discussed,[16-21] the precise behavior of ΔF is still uncertain. There are several reasons for deviations from Eq. (1), such as long-wavelength fluctuations of the interface between the liquid cluster and surrounding gas[6,14] corrections due to a dependence of f_I on $\delta\mu$,[4,12] the density difference between cluster and surrounding gas may differ from $\Delta\rho$ for small clusters[18,20] and their "typical" shape might be distinctly nonspherical.[16-21] It is not easy to resolve the uncertainties about ΔF, because there is some ambiguity concerning what is meant precisely by a "cluster."[19-24] Of course, there is no ambiguity in

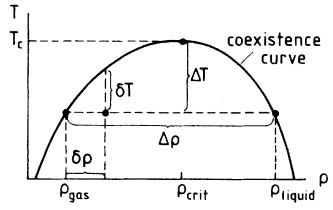

FIG. 1. Schematic phase diagram of a fluid. Below the coexistence curve, which terminates at the critical temperature T_c and critical density ρ_c, equilibrium requires two-phase coexistence.

considering the question at which rate unstable states decay[2,3,5] but since a direct solution of this problem of kinetics far from equilibrium does not yet exist, it is still useful to use nucleation theory concepts.

In the present work, an attempt is described to improve our knowledge of ΔF for the three-dimensional simple cubic lattice-gas model, with nearest-neighbor attractive interaction. We are mainly interested in the region close to the critical point, for several reasons: (i) T_c, the energy barrier $\Delta F/k_B T$ becomes a universal function of the relative supercooling $\delta T/\Delta T$ [or $\delta\rho/\Delta\rho$, cf. Fig. 1] (Ref. 3) and all three-dimensional liquid-gas systems as well as both fluid and solid binary mixtures should be described by the same function $\Delta F/k_B T_c = f(\delta T/\Delta T)$ as the lattice-gas model. (ii) Owing to critical slowing down[3,5] near T_c, one can observe experimentally[25–29] much larger relative supercoolings $\delta T/\Delta T$, which in turn correspond to smaller R/ξ, than far below T_c. (iii) Since ξ is very large near T_c, there is no difficulty in treating R as a continuous variable even if R/ξ is not very large, while far below T_c such a cluster would contain only a small total number of atoms.

In our approach, we study finite systems at supersaturated densities in which a stable two-phase equilibrium state is observed, extending previous work[4] on the two-dimensional lattice-gas model far below T_c. In Sec. II we introduce a new method for identifying cluster properties, which is much less hampered by any ambiguities in cluster definition than previous approaches. Section III describes the numerical results obtained from Monte Carlo simulations, while Sec. IV contains our conclusions.

II. TWO-PHASE EQUILIBRIA IN FINITE SYSTEMS

In the thermodynamic limit with total volume $V\to\infty$, a state which is a distance δT below the coexistence curve (Fig. 1) in thermodynamic equilibrium is a state consisting of two phases; i.e., macroscopic droplets of liquid density ρ_{liquid} will coexist with surrounding gas of density ρ_{gas}, the volume fraction of the fluid being given by $\delta\rho/\Delta\rho$ (see Fig. 1 for definitions). The chemical potential of such a state then is given by μ_{coex}, independent of $\delta\rho$ as long as $0<\delta\rho<\Delta\rho$, and the free energy of this state is given in terms of the double-tangent construction.

For finite V, this description is no longer true because now the interface between the coexisting

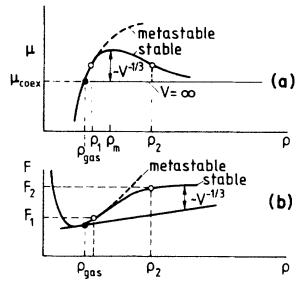

FIG. 2. Chemical potential (a) and free energy (b) plotted vs density near the gas branch of the coexistence curve, both for infinite and finite volumes (schematic). Dashed portions of the curves indicate metastable one-phase branches.

phases makes a contribution of order $V^{-1/3}$ to the average free-energy density (Fig. 2). Note that the volume taken by the minority phase is $\delta\rho V/\Delta\rho$ and hence there will be an interface area of the order of magnitude of $(\delta\rho/\Delta\rho)^{2/3}V^{2/3}$. The thermodynamic potential of such a mixed-phase state contains, hence, a bulk term proportional to V and an interfacial term proportional to $V^{2/3}$. The chemical potential $\mu\equiv(\partial F/\partial\rho)_{T,V}$ then is no longer constant but exhibits a loop, where again $\mu-\mu_{\text{coex}} \propto V^{-1/3}$. This behavior must not be confused with the approximate description of metastable states before droplets have been formed as done by van der Waals or Cahn-Hilliard equations,[12] where one-phase states are continued into the two-phase region for $V\to\infty$; the free energy of such states would be enhanced by an amount of order unity, independent of volume, in comparison with the equilibrium value.

It should also be noted that the region where F is a concave rather than convex function of ρ [and where $(\partial\mu/\partial\rho)_{T,V}$, hence, is negative] does not contradict the laws of thermodynamics, since these properties do not survive in the thermodynamic limit. In fact, since for finite systems the various thermodynamic ensembles are not strictly equivalent to each other,[30] there is also no problem with the stability of the system. This is illustrated in Fig. 3 where the relationship between μ and ρ in

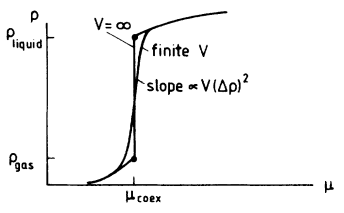

FIG. 3. Density plotted vs chemical potential (schematic, μVT ensemble).

the μVT ensemble (rather than the NVT ensemble of Fig. 2) is shown: The response function $(\partial\rho/\partial\mu)_{V,T}$ is everywhere positive.

Since $\mu(\rho,V,T)$ in Fig. 2(a) for finite V is a continuous function of ρ with a finite nonzero derivative $(\partial\mu/\partial\rho)_{T,V}|_{\rho_{gas}}$, it is clear that the density difference $\delta\rho_m=\rho_m-\rho_{gas}$ for which $\mu-\mu_{coex}$ reaches its maximum value ($\propto V^{-1/3}$) must also vanish for large V (proportional to $V^{-1/3}$). Hence, for large V there exists a regime of densities ρ_2 such that $\delta\rho_2=\rho_2-\rho_{gas}<<\Delta\rho$ but $\delta\rho_2>>\delta\rho_m$. In this regime, the equilibrium state is dominated by a configuration of the system, *containing just one*, nearly spherical, *droplet*. A typical configuration of the system, after some coarse-graining, will hence exhibit a density profile such as shown in Fig. 4(a). A droplet of size $R>>\xi$ will exist somewhere in the system and will be in equilibrium with surrounding gas. Since this state is an additive two-phase mixture which can exchange particles, the droplet and the surrounding gas must have the same chemical potential. As a consequence, the density of the surrounding gas is nothing else but the density ρ_1 at the one-phase branch of the μ-vs-ρ curve in Fig. 2(a). From this fact it follows that we find the total mass $M_{cluster}$ of the cluster in the case of Fig. 4(a) from the density difference $\rho_2-\rho_1$, which defines the effective cluster radius R,

$$M_{cluster}=V(\rho_2-\rho_1),\quad \frac{4\pi R^3}{3}\Delta\rho=M_{cluster}\ . \tag{2}$$

In this expression, we have neglected the difference between $\Delta\rho=\rho_{liquid}-\rho_{gas}$ and the actual density difference entering [Fig. 4(a)] $\Delta\rho'=\rho_{liquid}-\rho_1$.

As a result, knowledge of the function $\mu(\rho_2)$ for large V yields a relation between cluster radius R^* and chemical potential which is in equilibrium with that cluster size $R^*=R^*(\mu)$. Such a relation also is implied by any explicit phenomenlogical model. For example, from Eq. (1) the condition of having equilibrium $\partial(\Delta F_{class})/\partial R|_{R^*}=0$ yields

$$R^*_{class}(\mu)=2f_I/(\delta\mu\Delta\rho)\ . \tag{3}$$

In the general case, one may define an effective surface free energy F_l^{surf}, where $l\equiv\Delta\rho(4\pi R^3)/3$ denotes the cluster excess mass, in terms of the excess of the formation free energy over its volume term (see, e.g., Ref. 4)

$$\Delta F\equiv -l\delta\mu+F_l^{surf}\ ; \tag{4}$$

the condition of having equilibrium $\partial(\Delta F)/\partial l|_{l^*}=0$ then yields[31]

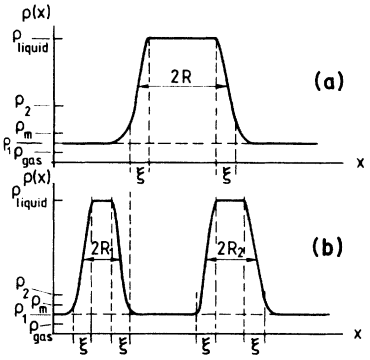

FIG. 4. Typical coarse-grained density profile in one coordinate direction x, for coordinates y,z identical to the respective center-of-gravity coordinates of the cluster, for $\rho_2>>\rho_m$ (a) and $\rho_2\gtrsim\rho_m$ (b). In the latter case, the center-of-gravity coordinates of both clusters in y and z directions have, for simplicity, been assumed to coincide.

$$(\partial F_l^{surf}/\partial l)_T|_{l^*}=\delta\mu\ . \tag{5}$$

Now the equilibrium between the liquid droplet and the surrounding box, which is considered here, is not an equilibrium at constant chemical potential $\delta\mu$—as is well known, this would be an unstable equilibrium—but it is an equilibrium at constant *total* particle number: After all, this fact is responsible for having a stable equilibrium, under conditions investigated in Ref. 4. This work also showed that the "Kelvin equation," Eq. (3), or its generalization, Eq. (5), still are valid in spite of the fact that we consider a constant ρ rather than constant μ ensemble.

Nevertheless, it is important to pay attention to systematic errors which may arise since one is trying to exploit rather small differences between the behavior of a finite system and the infinite system (Fig. 2). There are three types of effects: (i) Close to the critical point the correlation length ξ diverges. Hence it is necessary to choose the linear dimension $V^{1/3}$ of the system such that $V^{1/3}>>\xi$. Even then finite-size corrections of order $\exp(-V^{1/3}/\xi)$ may occur. Since we are already interested in the regime $R>>\xi$ and must have[32] $R<<V^{1/3}$, on the other hand, the finite-size corrections of order $\exp(-V^{1/3}/\xi)$ are expected to be negligibly small. (ii) While Eqs. (3) and (5) describe the average thermal equilibrium, it is clearly important to also consider fluctuations around this equilibrium. In Ref. 4 it was shown that the second derivative of the total free energy of the system with respect to cluster excess mass l is

$$\left[\frac{\partial^2 F}{\partial l^2}\right]_{N,V,T}\Bigg|_{l=l^*} \cong \left[\frac{\partial^2 F_l^{\rm surf}}{\partial l^2}\right]_T\Bigg|_{l=l^*} + \chi_G^{-1} V^{-1} , \tag{6}$$

where

$$\chi_G \equiv -(1/V)(\partial^2 \Omega/\partial \mu^2)_{T,V,\mu=\mu_{\rm coex}}$$

is the second derivative of the grand-canonical potential $\Omega(T,V,\mu)$ at the gas branch of the coexistence curve. In the limit where l is large and Eq. (1) can be applied, we have

$$F_l^{\rm surf} = (36\pi)^{1/3} f_I (l/\Delta\rho)^{2/3}$$

and since $l = \delta\rho V$, it follows that

$$(\partial^2 F_l^{\rm surf}/\delta l^2)_T \,|_{l=l^*} \cong -(32\pi/81)^{1/3} f_I (\delta\rho/\Delta\rho)^{-4/3} V^{-4/3} .$$

As a consequence, the relative mean-square fluctuation of l is

$$(\overline{l^2} - \bar{l}^2)/\bar{l}^2 = k_B T [(\delta^2 F/\partial l^2)_{N,V,T} \,|_{l=l^*}]^{-1}/\bar{l}^2$$
$$= \chi_G (\Delta\rho/\delta\rho)^2 V^{-1}/[1 - (32\pi/81)^{1/3} f_I (\delta\rho/\Delta\rho)^{-4/3} \chi_G V^{-1/3}]. \tag{7}$$

Thus, although the relative fluctuation decreases asymptotically proportional to the inverse volume as in usual thermal averaging, the coefficient of this V^{-1} law is very large, since χ_G diverges near T_c as $\xi^{\gamma/\nu}$, $\Delta\rho/\delta\rho$ is also much larger than unity, and the denominator in Eq. (7) typically is much less than unity also.

These large fluctuations make a successful sampling of cluster size by Monte Carlo methods very difficult if one tries to obtain $\bar{l}$ by direct observation as described in Ref. 4. In the present work, where $l^* = \Delta\rho(4\pi R^{*3}/3)$ is defined in terms of given total densities, ρ_1, ρ_2 and hence not fluctuating, instead it is the chemical potential μ which is the statistically fluctuating quantity to be sampled. For three-dimensional systems, the quantity of interest which is the excess $\bar{\mu} - \mu_{\rm coex} \propto V^{-1/3}$ does exceed the fluctuation of μ, $(\overline{\mu^2} - \bar{\mu}^2)^{1/2} \propto V^{-1/2}$ and hence the distribution of μ values does sharpen up as V is increased, although much slower than usual: We find

$$(\overline{\mu^2} - \bar{\mu}^2)^{1/2}/(\bar{\mu} - \mu_{\rm coex}) \propto V^{-1/6} .$$

As a result the Monte Carlo sampling of $\mu - \mu_{\rm coex}$ will be difficult. For the two-dimensional case studied in Ref. 4, the excess $\bar{\mu} - \mu_{\rm coex} \propto V^{-1/2}$ is of the same order as the fluctuation, and thus the distribution becomes even "volume independent." Similar properties are found with respect to the interface free energy of the system, which is of order $V^{2/3}$ in three and $V^{1/2}$ in two dimensions, while the fluctuations of the bulk free energy are of order $V^{1/2}$.

Nevertheless, the present method of studying two-phase coexistence in a finite three-dimensional volume is a potentially very powerful method for studying properties of large clusters, if one could apply analytic methods (such as renormalization-group approaches) where one would not be hampered by the above fluctuations. In addition, one would obtain the free energies F_1, F_2 directly [Fig. 2(b)], and hence one could get the cluster formation free energy ΔF rather directly. In a Monte Carlo sampling, one can obtain the free-energy difference from thermodynamic integration $F_2 - F_1 = \int_{\rho_1}^{\rho_2} \mu \, d\rho$, but this method sometimes is hampered by hysteresis effects in the curve $\mu(\rho)$ near ρ_m, where, due to short observation time, the data often follow the metastable one-phase branch rather than the stable one [Fig. 2(a)], at least at low temperatures (Sec. III).

(iii) The most serious limitation is important for R/ξ not very large where a systematic error in Eq. (2) is introduced, because not just only states with one cluster [Fig. 4(a)] contribute to the averaging, but also states with two or more clusters [Fig. 4(b)] contribute as well. Of course, if the mass $M_{\rm cluster}$ is partitioned into two clusters with radii R_1, R_2 such that $R_1^3 + R_2^3 = R^3$, the total interface $4\pi(R_1^2 + R_2^2)$ exceeds that of $4\pi R^2$ (for at most a factor of $2^{1/3}$, in the case $R_1 = R_2$). These states hence cost much more interface energy, but they have more entropy due to the arbitrary choice of R_1/R_2 and relative positions of the clusters. Thus, states with several clusters will become important for R/ξ not much larger than unity, i.e., for densities ρ_2 close to ρ_m. There the state of the system changes completely gradually to one-phase states, where the density of clusters of size $R/\xi \approx 1$ (i.e., homophase instead of heterophase fluctuations, see also Refs. 19 and 20), is somewhat enhanced in comparison with one-phase states at the coexistence curve. The situation can be understood in terms of fluctuations in the interface area

(Fig. 5). For $\rho_2 \gg \rho_m$, the cluster is very large, and the fluctuations with low free-energy cost are similar to capillary waves, i.e., the long-wavelength fluctuations considered for flat interfaces[15] [Fig. 5(a)]. It is believed that these fluctuations give rise to the leading corrections to Eq. (1) for large R.[6,14] As ρ_2 becomes smaller, the distortions of the interface are no longer small-amplitude fluctuations, and hence the actual cluster shapes are strongly nonspherical (although the *average* density profile in the cluster center-of-gravity system is spherical for temperatures near T_c) [Fig. 5(b)]. The effect of these strong fluctuations, which is hard to analyze by the analytical techniques of Refs. 6 and 14, has led to considerable discussion in the literature (e.g., Refs. 2–4 and 16–21). The effect of these fluctuations on the "effective surface free-energy" $F_l^{\rm surf}$ and the resulting free-energy barrier is one of the central interests of this paper. Finally, for ρ_2 near ρ_m the fluctuations in interface area are so large that the cluster occasionally splits into parts [Fig. 5(c)] and recombines, and then a clear-cut relation between the function $\delta\mu(\rho)$ and properties of single clusters is lost. Thus the following numerical analysis will be restricted to the regime $R/\xi \gtrsim 3$, where $\rho_2 - \rho_{\rm coex} >> \rho_m - \rho_{\rm coex}$.

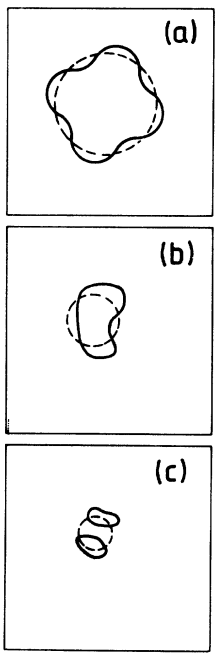

FIG. 5. Typical cluster shapes (full curves) as compared to minimum interface shapes (dashed circles) for $\rho_2 > > > \rho_m$ (a), $\rho_2 >> \rho_m$ (b), and $\rho_2 \gtrsim \rho_m$ (c) (schematic).

III. NUMERICAL RESULTS FOR THE SIMPLE CUBIC NEAREST-NEIGHBOR LATTICE GAS MODEL

We performed Monte Carlo simulations for the temperatures $k_B T/J = 2,3,4,4.2,4.3,4.4$ [note $k_B T_c/J \approx 4.51$ (Ref. 33)], using lattice linear dimensions $V^{1/3} = 4$, 6, 8, 10, 15, 18, 24, and 36 (this largest lattice size was used at the temperature closest to T_c only, and only a subset of these linear dimensions was used at each temperature), applying periodic boundary conditions. In order to prepare initial states at a given density ρ, we put a mass $V(\rho - \rho_{\rm gas})$ into a cluster in the center of the box while the atoms representing the remaining mass $V\rho_{\rm gas}$ were distributed randomly in the remaining volume. This initial condition favors a two-phase equilibrium state. The value of the density at the coexistence curve ($\rho_{\rm gas}$) was estimated from the low-temperature expansions for the magnetization M of the Ising model,[33] using $\rho_{\rm gas} = (1-M)/2$. For small values of ρ we also use a second initialization where *all* atoms are distributed randomly in the volume, thus favoring a one-phase state. These two different initializations enable us to check for hysteresis effects near ρ_m [Fig. 2(a)].

Equilibrium then was obtained in the standard way of performing Monte Carlo calculations at constant density, using the Kawasaki nearest-neighbor pair exchange technique.[34,35] Even though our initial states are already in a sense "close" in phase space to the equilibrium states, equilibration was a rather slow process since particles typically had to "evaporate" from the central cluster and diffuse out into the gas region, until one achieved the correct equilibrium between the cluster (at liquid density close to $\rho_{\rm liquid}$ rather than the initial maximum density $\rho = 1$) and surrounding gas (at density $\rho_1 > \rho_{\rm gas}$, cf. Fig. 2). Since atoms have to diffuse a distance of order $L \approx V^{1/3}/2$, we conclude that the time in order to reach equilibrium is at least of order $t = L^2/6D \approx V^{2/3}/(24D)$, where D is the diffusion constant [which is much less than unity if one uses one Monte Carlo step (MCS) per atom as a time unit]. Thus we have omitted typically the first 1000 MCS per site from the averaging which then typically was extended over 6000 MCS per atoms. Very close to T_c even larger times were used.

The data for the chemical potential thus obtained are shown in Figs. 6 and 7. The chemical potential μ in Monte Carlo simulation at constant density is obtained from a method proposed by

Meirovitch and Alexandrowicz.[36] There one samples the frequencies ν_α of the local states α (of energy E_α) of each lattice site, using the formula[36]

$$\mu/k_BT=\frac{1}{7}\sum_{\alpha=1}^{7}[\ln(\nu_\alpha/\nu_{\alpha'})+E_\alpha/k_BT] .$$

These seven local states are the states where a site has between zero and six neighboring sites occupied. Note also that $\mu_{\text{coex}}=-12J$ in the simple cubic Ising lattice-gas model. It is seen that the function $\mu(\rho)$ has, indeed, the general structure as predicted in Fig. 2(a). Hysteresis due to metastable one-phase states was only clearly established at the two lowest temperatures (Fig. 6).

For $k_BT/J=2.0$ we also have used the method of Ref. 4, where clusters in the system were identified as groups of atoms connected by nearest-neighbor atoms (Fig. 8). Such a cluster identification becomes meaningless at higher temperatures, where a "percolating" cluster would appear extending throughout the lattice.[37] From such a direct observation of the configuration one obtains the average size $\bar{l}$ of the (largest) cluster in the system, and also checks that during the time of observation, this cluster keeps its identity (i.e., it does not split into several parts of comparable size nor does any other cluster of similar size form by nucleation). The resulting relation $\mu=\mu(\bar{l})$ is in reasonable agreement with the relation obtained,

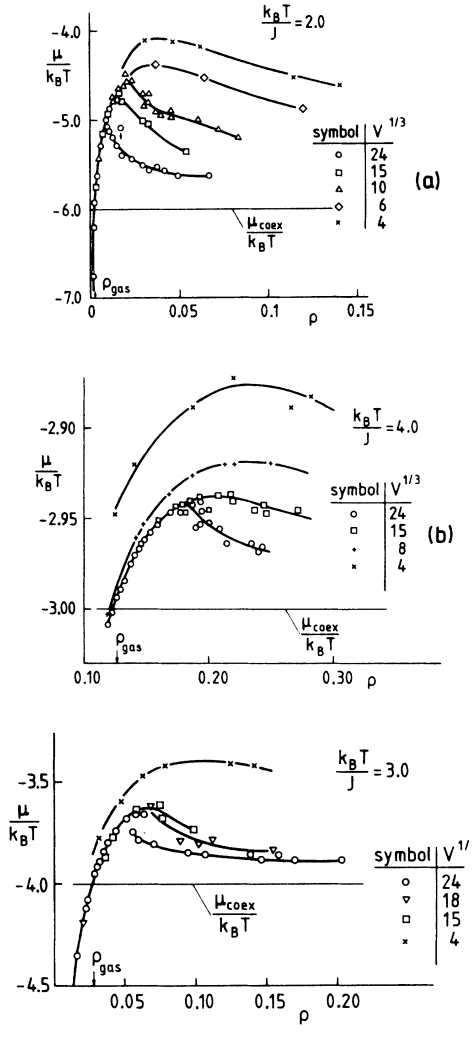

FIG. 6. Chemical potential plotted vs density for $k_BT/J=2$ (a), 3 (b), and 4 (c). Monte Carlo data for various values of V are shown. Point with arrow in Fig. 2(a) shows a slowly relaxing metastable one-phase state. Curves are drawn to guide the eye only.

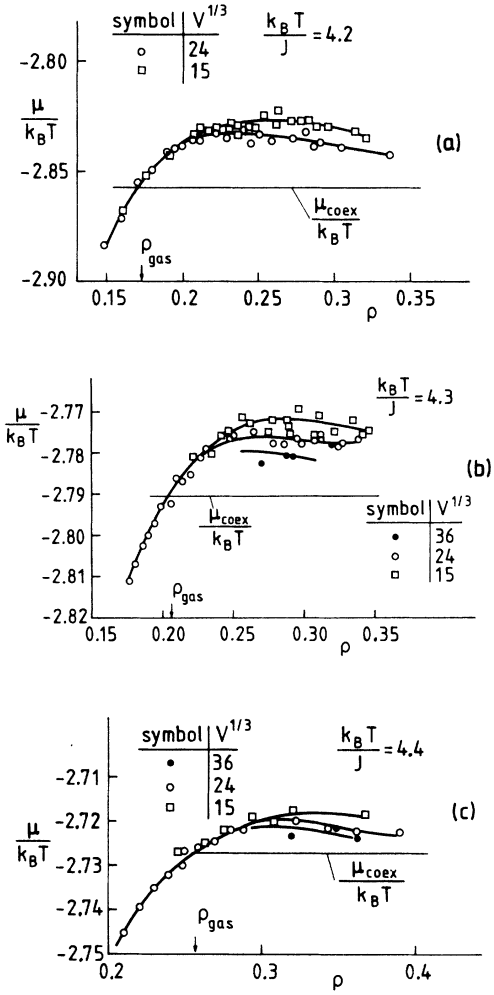

FIG. 7. Chemical potential plotted vs density for $k_BT/J=4.2$ (a), 4.3 (b), and 4.4 (c). Monte Carlo data for various values of V are shown. Curves are drawn to guide the eye only.

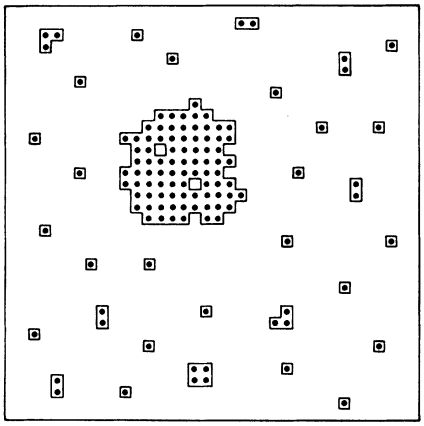

FIG. 8. Snapshot picture of atomic configuration in a two-dimensional system, indicating the definition of clusters in terms of contours around groups of atoms connected by nearest-neighbor bonds (schematic).

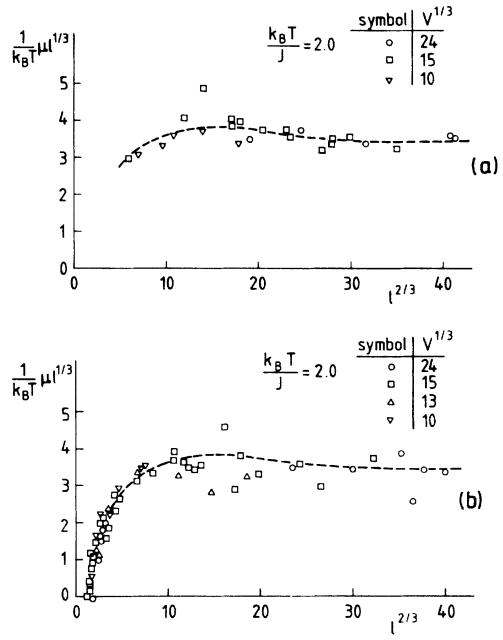

FIG. 9. Plot of the quantity $(\delta\mu/k_BT)l^{1/3}$ vs $l^{2/3}$ where μ and l were obtained from the relation $\mu(\rho)$ as indicated in Eq. (2) (a) and from the direct observation of largest clusters (b) at $k_BT/J=2$. Note that the same curve fits both sets of data.

where $l=\Delta\rho(4\pi R^3/3)$ was found from Eq. (2) (see Fig. 9). Since we expect from Eq. (3) for large l that $\delta\mu \propto l^{-1/3}$, we have plotted the quantity $\delta\mu l^{1/3}/k_BT$, which should tend towards the constant $2(4\pi/3)^{1/3}f_I/k_BT$ for large l. The Monte Carlo data are indeed consistent with this behavior; $\delta\mu l^{1/3}/k_BT$ seems to be significantly smaller than this constant only for values of l as small as $l=10$.

The data closer to T_c have been represented in similar form, but we here normalize our data such that they bring out clearly the expected scaling and universality behavior. Defining $x=(2/\beta)(\delta\rho/\Delta\rho)$, where β is the critical exponent of the order parameter [$\Delta\rho=B(1-T/T_c)^{\beta}$], it follows from Eqs. (1) and (3) that the nucleation energy barrier can be expressed in the form

$$\Delta^*_{\text{class}}/k_BT_c=x_0^2/x^2\ , \tag{8}$$

where

$$[f_I=\hat{f}_I(1-T/T_c)^{2\nu},(\partial\rho/\partial\mu)_T=C_-(1-T/T_c)^{-\gamma}/4,3\nu=\gamma+2\beta],\quad x_0^2=\frac{64\pi}{3\beta^2}\frac{f_I^3(\partial\rho/\partial\mu)_T^2}{k_BT_c(\Delta\rho)^4}=\frac{16\pi}{3\beta^2}\hat{f}_I^3\frac{C_-^2}{B^4}\ . \tag{9}$$

The constant x_0 should be universal; estimates for it are in the range from $x_0=1.14\pm0.10$ (Ref. 38) to $x_0=1.30\pm0.10$.[5] Thus, instead of $\delta\mu l^{1/3}/k_BT$, we plot in Fig. 10 the quantity

$$\frac{\delta\mu l^{1/3}}{k_BT_c}\left[\frac{k_BT(\partial\rho/\partial\mu)_T\sqrt{2}}{\beta\Delta\rho}\right]^{2/3}\underset{l\to\infty}{\longrightarrow}x_0^{2/3}\ , \tag{10}$$

and as an abscissa we choose $(R/\xi)^2$ [where $\xi=f_1^-(1-T/T_c)^{-\nu}$; the amplitude f_1^- is taken from Ref. 39], since then all temperatures in the critical region should fall on the same (universal) curve. Within the (unfortunately rather large) statistical scatter of the Monte Carlo data, this scaling behavior seems indeed to hold. The quantity $\delta\mu l^{1/3}/k_BT_c$ can be considered as the derivative of the effective interface free energy F_l^{surf} with respect to the effective interface area: From Eq. (5) and $l=(4\pi/3)R^3/\Delta\rho$, one finds

$$\delta\mu=(\partial F_{\text{surf}}/\partial l)_{l^*}=(\partial F_{\text{surf}}/\partial R^2)_{R^*}(\partial R^2/\partial l)_{l^*}$$

and hence

$$\left[\frac{\partial F_l^{\text{surf}}}{\partial R^2}\right]_{R^*}=2\pi\Delta\rho R\,\delta\mu$$

$$=2\pi\left[\frac{3(\Delta\rho)^2}{4\pi}\right]^{1/3}\delta\mu l^{1/3}\ . \tag{11}$$

From Eq. (1), on the other hand, one would find $\partial F_l^{\rm surf}/\partial R^2 = 4\pi f_I$, i.e., a constant derivative independent of R. Some data points for large (R/ξ) seem to fall systematically above the range of values within which the scaled derivative of the surface free energy is expected to occur for $R/\xi \to \infty$ (the boundaries of this range are given by the dash-dotted straight lines). Since most of these data points refer to a temperature distinctly below $T_c(k_BT/J=3)$, we expect that this effect is due to corrections for the leading asymptotic scaling behavior close to T_c. In fact, far below T_c the anisotropy of the surface tension in lattice gases is known to be rather important; it leads to cluster shapes more resembling a cubic shape rather than a spherical one.[40] This effect leads to an enhancement of the surface free energy in comparison to what one would expect according to the present treatment.

From Fig. 10 it is seen, however, that this derivative for $(R/\xi)^2 \lesssim 20$ is distinctly smaller than its asymptotic value for large R/ξ. From Figs. 2 and 9 it is clear that near $\mu_m \equiv \mu(\rho_m)$ we have $\mu_m - \mu \propto (\rho - \rho_m)^2 \propto l^2$, and hence there

$$\delta\mu l^{1/3} \approx (\mu_m - \mu_{\rm coex}) l^{1/3} ,$$

which implies that the curve plotted in Fig. 10 starts out at the origin with a square-root-like behavior $\delta\mu l^{1/3} \propto \sqrt{x}$, where $x = (R/\xi)^2$. Owing to the fact that near ρ_m the state of the system changes from a state with a single large cluster to a state with many smaller clusters (Fig. 5), the behavior of $\Delta\mu l^{1/3}$ for small x is *no longer related to the interface free energy of "single" clusters.* In other words, the variable R has the meaning of a (single) cluster radius only for R distinctly larger than ξ. For $(R/\xi)^2 << 10$, for example, nothing can be inferred from Fig. 10 concerning the actual surface free energy of clusters. Of course, this inaccessible region $(R/\xi)^2 \lesssim 10$ is not of direct experimental interest even. Nevertheless, the variables of l and R are mathematically still well defined even in this regime, and hence Eq. (11) can be used to find the surface free energy $F_l^{\rm surf}$ itself by thermodynamic integration,

$$F_l^{\rm surf} = \int_0^{R^2} (\partial F_l^{\rm surf}/\partial R^2) dR^2 = 2\pi\xi^2 \left[\frac{3(\Delta\rho)^2}{4\pi}\right]^{1/3} \int_0^{(R/\xi)^2} \delta\mu l^{1/3} dx \ . \qquad (12)$$

Figure 11 shows the resulting surface free energy in comparison with the corresponding classical prediction,

$$\left[\frac{F_l^{\rm surf}}{k_BT_c}\right]_{\rm class} = \frac{4\pi \hat{f}_I (f_1^-)^2}{k_BT_c}\left[\frac{R}{\xi}\right]^2 = \frac{4\pi (f_1^-)^2}{k_BT_c}\left[\frac{3\beta^2 B^4 x_0^2}{16\pi C_-^2}\right]^{1/3}\left[\frac{R}{\xi}\right]^2 . \qquad (13)$$

Although there is some uncertainty about the prefactor in this relation, due to the uncertainty in the constant x_0 mentioned above, it seems clear from our data that the actual $F_l^{\rm surf}$ falls distinctly below the classical capillarity approximation $(F_l^{\rm surf})_{\rm class}$ in the range of interest $20 \lesssim (R/\xi)^2 \lesssim 50$.

Finally, we emphasize that although we have to include the region of small R/ξ for which we cannot obtain $F_l^{\rm surf}$ itself, in the integral equation (23) also for large R/ξ, no systematic error is thereby

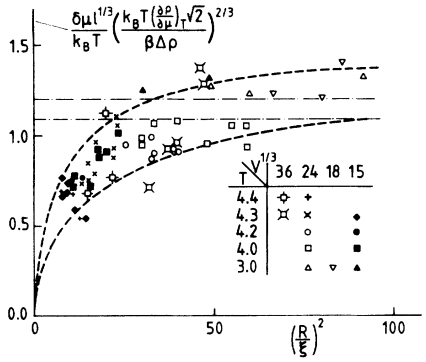

FIG. 10. Plot of the scaled derivative of the effective interface free energy with respect to the scaled effective interface area $(R/\xi)^2$ vs $(R/\xi)^2$; various temperatures and volumes are shown. Straight dash-dotted lines correspond to $x_0^{2/3} \simeq 1.09$ (Ref. 37) and $x_0^{2/3} \approx 1.20$ (Ref. 5). Broken curves indicate two extreme choices for the scaled derivative.

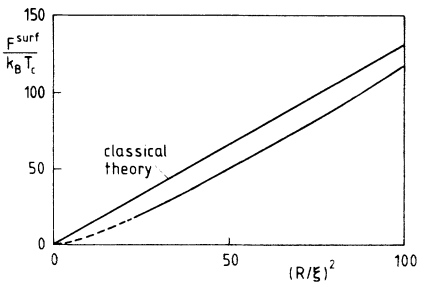

FIG. 11. Surface free energy F_{l^*}/k_BT_c plotted vs $(R/\xi)^2$, as obtained from the data in Fig. 10 [via Eq. (12)] and from classical capillarity approximation, Eq. (13), with $x_0^{2/3} = 1.15[=(1.09+1.20)/2]$. Plotted curve for F_{l^*}/k_BT_c is the average of the two functions obtained from integrating the broken curves in Fig. 10.

introduced (see Appendix). Using the numerical results of Fig. 11 together with Eq. (5), one readily obtains the formation free energy ΔF of the clusters as a function of their effective radius. Since each cluster radius corresponds to a definite value of $\delta\mu$ due to the equilibrium condition Eq. (5), and since $\rho_2-\rho_{\rm gas}=\delta\mu(\partial\rho/\partial\mu)_T$ for small $\delta\mu$, we can express our results for ΔF in a form similar to Eq. (8), where the energy barrier is expressed as a function of $(\rho_2-\rho_{\rm gas})/\Delta\rho$. This choice of variables is motivated by the fact that, in a system with macroscopic volume (where the equilibrium between a critical cluster surrounding supersaturated gas is an unstable one, of course),[4] the density of the gas surrounding the critical clusters (ρ_1) is practically the same as the total density ρ (Fig. 1), at least for the case where $\Delta F/k_BT_c$ is very large and the concentration of critical clusters [which varies as $\exp(-\Delta F/k_BT_c)$] would be negligibly small. Thus Fig. 12 shows $\Delta F/k_BT_c$ plotted versus x^{-2} in order to compare our results to Eq. (8). It is seen that the energy barrier for $x^{-2}\approx 10-30$ (to which the data recorded in Figs. 10 and 11 correspond) are distinctly smaller than what one would expect according to classical theory. This behavior is not so surprising, since $x=1$ corresponds to $\delta\rho/\Delta\rho=\beta/2\approx 0.16$, i.e., a density far away from the coexistence curve, which already belongs to the regime where spinodal decomposition occurs.[3,12] In fact, according to the mean-field (or Ginzburg-Landau) theory, where $\beta=\frac{1}{2}$ one would predict[12] that ΔF vanishes at a spinodal curve, which would be located at $\delta\rho_s/\Delta\rho=(1-1/\sqrt{3})/2\approx 0.21$; this value would correspond to $x^{-2}\approx 1.4$. Since one expects that the actual transition from nucleation to spinodal decomposition occurs much closer to the coexistence curve than predicted by the mean-field theory, it is reasonable to locate it for x^{-2} of order 10^1. It has been emphasized[3] that a sharp spinodal line where $\Delta F/k_BT_c$ vanishes does not exist; rather one expects a gradual transition from nucleation ($\Delta F/k_BT_c >> 1$) to spinodal decomposition ($\Delta F/k_BT_c$ is small and hence no longer meaningful). While classical nucleation theory hardly shows this transition at all [note that it is not meaningful to consider values of x of order unity for which $\Delta F/k_BT_c$ according to Eq. (8) would be small], this transition is clearly exhibited by the present work. Our numerical results (Fig. 12) confirm qualitatively— but not quantitatively—the predictions of the Cahn-Hilliard theory[12] and a calculation[3] based on Fisher's droplet model,[16] according to which $\Delta F/k_BT_c$ is below its classical value in the range $20<\Delta F/k_BT_c<50$; unfortunately, both the precise quantitative amount of this energy barrier reduction and the analytic form of $\Delta F/k_BT_c$ in this regime remain rather uncertain.

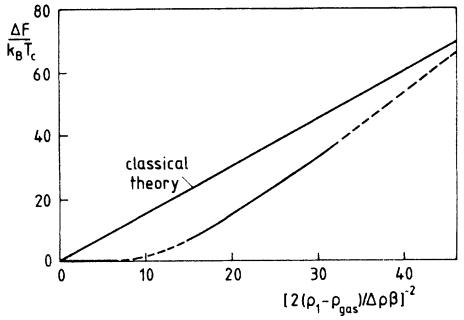

FIG. 12. Energy barrier F_{l^*}/k_BT_c against nucleation plotted vs the variable x^{-2}, where $x=2(\rho_1-\rho_{\rm gas})/(\beta\Delta\rho)$. The straight line is the result of the classical capillarity approximation, Eq. (8), using $x_0^{2/3}=1.15$, while the full curve is the result of the present calculation (dashed portions are tentative extrapolations).

IV. CONCLUSIONS

In this study, the surface free-energy contribution occurring in two-phase equilibria in systems with a finite volume V was investigated. It was argued that the chemical potential differed in the two-phase region from its value at the coexistence curve by a contribution of order $V^{-1/3}$. This interfacial contribution can be used to estimate the derivative of the interface free energy of clusters with respect to the effective cluster area. It is shown that this quantity is consistent with the expected scaling properties near the critical point and tends towards the expected universal constant ($x_0^{2/3}$) for large cluster volumes. For intermediate cluster sizes [$20\lesssim(R/\xi)^2\lesssim 100$, where ξ is the correlation length] this derivative, as well as the surface free energy itself, seems to be somewhat smaller than that according to what one would expect from classical nucleation theory. This reduction is interpreted in terms of a transition to the spinodal regime in the vicinity of $\delta\rho/\Delta\rho\approx 0.05$.

Unfortunately, the present results can hardly be used to establish the precise analytic form of corrections to the classical nucleation theory. Partly this is due to the rather limited statistical accuracy of the data, which is inevitable in view of the relatively large fluctuations of the excess chemical potential, and partly is due to imprecise knowledge of the constant x_0, which enters into the prefactor of the scaled interface energy in classical nu-

cleation theory. It is hoped, however, that this work will stimulate related studies with more powerful techniques rather than the Monte Carlo methods applied here, which then could narrow down these uncertainties. More precise experimental studies of nucleation barriers in the critical region also would be highly desirable. The quicker decrease of $\Delta F/k_B T_c$ with increasing supersaturation (Fig. 12) than that predicted according to classical nucleation theory should reduce the relative supercooling $\delta T/\Delta T$ close to T_c. Taking such effects into account might improve the agreement of calculations such as Ref. 5 with experiment (Refs. 28 and 29).

ACKNOWLEDGMENTS

One of us (K. B.) thanks W. Klein and D. Stauffer for discussions.

APPENDIX: THERMODYNAMIC INTEGRATION METHOD FOR THE CLUSTER SURFACE FREE ENERGY

In this appendix we derive Eq. (12) in a different way, establishing that the physical nature of the states near ρ_m is irrelevant for the validity of Eq. (12) for states at densities $\rho_2 >> \rho_m$ (Fig. 2). We start from the relation for the free energy per unit volume $\mu \equiv \{ \partial F(\rho,T)/\partial\rho \}_T$, which is integrated as

$$F(\rho_2)=F(\rho_1)+\int_{\rho_1}^{\rho_2}\mu\, d\rho \ .$$

Since the state at density ρ_2 is a two-phase state where a volume fraction $1-l/\Delta\rho V$ is taken up by gas of density ρ_1 and the rest by the liquid cluster, additivity of thermodynamic potentials yields

$$F(\rho_2)=F(\rho_1)\left[1-\frac{l}{\Delta\rho V}\right]+\frac{1}{V}F_{\text{cluster}},\quad F_{\text{cluster}}=\frac{l}{\Delta\rho}F(\rho_2)+V\int_{\rho_1}^{\rho_2}\mu\, d\rho \ , \tag{A1}$$

where F_{cluster} is the total free energy of the cluster. The bulk part of the liquid free energy at the coexistence curve is, from the double-tangent construction, $F_{\text{cluster}}^{\text{coex}}=(l/\Delta\rho)[F(\rho_{\text{gas}})+\mu_{\text{coex}}\Delta\rho]$. The formation free energy of a cluster is then obtained from the difference

$$\Delta F=F_{\text{cluster}}-F_{\text{cluster}}^{\text{coex}}=\frac{l}{\Delta\rho}[F(\rho_1)-F(\rho_{\text{gas}})]+V\int_{\rho_1}^{\rho_2}\mu\, d\rho-l\mu_{\text{coex}} \ . \tag{A2}$$

Since $l=V(\rho_2-\rho_2)$, one can rewrite Eq. (2) as

$$\Delta F=\frac{l}{\Delta\rho}[F(\rho_1)-F(\rho_{\text{gas}})]+V\int_{\rho_1}^{\rho_2}\delta\mu\, d\rho=\frac{l}{\Delta\rho}[F(\rho_1)-F(\rho_{\text{gas}})]+F^{\text{surf}} \ , \tag{A3}$$

where the interfacial free energy of the cluster is found as

$$F_l^{\text{surf}}=V\int_{\rho_1}^{\rho_2}\delta\mu\, d\rho \ . \tag{A4}$$

This expression only requires that $\delta\mu(\rho_1)=\delta\mu(\rho_2)$ is small, i.e., $\rho_2 >> \rho_m$. It is not hampered by any uncertainty about the physical nature of states near ρ_m. Equation (4) is equivalent to Eq. (12), since $dl=V(d\rho_2-d\rho_1)$, and hence [the variable x in Eq. (12) is proportional to $l^{2/3}$]

$$F_l^{\text{surf}}=\tfrac{3}{2}\int_0^l\delta\mu l^{1/3}d(l^{2/3})=\int_0^l\delta\mu\, dl=V\left[\int_{\rho_m}^{\rho_2}\delta\mu\, d\rho-\int_{\rho_m}^{\rho_1}\delta\mu\, d\rho\right]=V\int_{\rho_1}^{\rho_2}\delta\mu\, d\rho \ . \tag{A5}$$

---

*Present and permanent address: Faculty of Education, Yamaguchi University, Yamaguchi 753, Japan

[1]For recent reviews, see J. S. Langer, in *Systems Far from Equilibrium,* edited by L. Garrido (Springer, Berlin, 1980), and Refs. 2 and 3. Earlier work is reviewed in Refs. 8–10.

[2]K. Binder, J. Phys. (Paris) 41, C4–51 (1980).

[3]K. Binder and D. Stauffer, Adv. Phys. 25, 343 (1976).

[4]K. Binder and M. H. Kalos, J. Stat. Phys. 22, 363 (1980).

[5]J. S. Langer and A. J. Schwartz, Phys. Rev. A 21, 948 (1980).

[6]N. J. Günther, D. A. Nicole, and D. J. Wallace, J. Phys. A 13, 1755 (1980).
[7]R. McGraw and H. Reiss, J. Stat. Phys. 20, 385 (1979).
[8]*Nucleation* edited by A. C. Zettlemoyer (Dekker, New York, 1969); *Nucleation Phenomena,* edited by A. C. Zettlemoyer (Elsevier, New York, 1977).
[9]F. F. Abraham, *Homogeneous Nucleation Theory* (Academic, New York, 1974).
[10]J. Feder, K. C. Russell, J. Lothe, and G. M. Pound, Adv. Phys. 15, 117 (1966).
[11]J. S. Langer and L. A. Turski, Phys. Rev. A 8, 3230 (1973); K. Kawasaki, J. Stat. Phys. 12, 365 (1975).
[12]J. W. Cahn and J. E. Hilliard, J. Chem. Phys. 28, 258 (1958); 31, 688 (1959).
[13]A. Eggington, C. S. Kiang, D. Stauffer, and G. H. Walker, Phys. Rev. Lett. 26, 820 (1971); C. S. Kiang, D. Stauffer, G. H. Walker, O. P. Puri, T. D. Wise, Jr., and E. M. Patterson, J. Atmos. Sci. 28, 1112 (1971); P. Hamill, C. S. Kiang, and D. Stauffer, Chem. Phys. 28, 209 (1974).
[14]J. S. Langer, Ann. Phys. (N.Y.) 54, 258 (1969); 41, 108 (1967).
[15]B. Widom, in *Phase Transitions and Critical Phenomena,* edited by C. Domb and M. S. Green (Academic, New York, 1972), Vol. II.
[16]M. E. Fisher, Physics (N.Y.) 3, 255 (1967).
[17]D. Stauffer, C. S. Kiang, and G. H. Walker, J. Stat. Phys. 3, 323 (1971); see also L. P. Kadanoff, in *Critical Phenomena,* edited by M. S. Green (Academic, New York, 1971).
[18]K. Binder, D. Stauffer, and H. Müller-Krumbhaar, Phys. Rev. B 12, 5261 (1975).
[19]K. Binder, Ann. Phys. (N. Y.) 98, 390 (1976).
[20]R. Kretschmer, K. Binder, and D. Stauffer, J. Stat. Phys. 15, 267 (1976).
[21]C. Domb, J. Phys. A 9, 283 (1976).
[22]A. Coniglio and W. Klein, J. Phys. A 13, 2775 (1980).
[23]D. Stauffer, J. Phys. (Paris) Colloq. 42, L99 (1981); J. Roussenq, J. Aerosol Sci. 12, No. 6 (1981).
[24]D. J. Wallace and A. D. Bruce, Phys. Rev. Lett. 47, 1743 (1981).
[25]R. B. Heady and J. W. Cahn, J. Chem. Phys. 58, 896 (1973).
[26]D. Dahl and M. R. Moldover, Phys. Rev. Lett. 27, 1421 (1971).
[27]J. S. Huang, W. I. Goldburg, and M. R. Moldover, Phys. Rev. Lett. 34, 639 (1975).
[28]A. J. Schwartz, S. Krishnamurthy, and W. I. Goldburg, Phys. Rev. 22, 2147 (1980).
[29]R. G. Howland, N. Wong, and C. M. Knobler, J. Chem. Phys. 73, 522 (1980).
[30]T. L. Hill, *Thermodynamics of Small Systems* (Benjamin, New York, 1963/1964).
[31]Note that in Ref. 4 the symbol l stands for particle number rather than excess mass of the cluster; hence Eq. (32) of Ref. 4, which corresponds to the present Eq. (5), contains an additional factor $1-\rho_{\text{gas}}/\rho_{\text{liquid}}$.
[32]The condition $R << V^{1/3}$ is necessary since, due to the periodic boundary condition in the system, the configuration with minimum interface area is that of a domain with two flat interfaces (of area $V^{2/3}$ each) for densities ρ_2 exceeding a density ρ_2^c corresponding to a radius R_c [Eq. (2)] which is given by $4\pi R_c^2=2V^{2/3}$, $R_c=(2\pi)^{-1/2}V^{1/3}$. Even for R somewhat smaller than R_c fluctuations in which such a state with flat interfaces instead of a spherical domain are formed, and which correspond to $\delta\mu\approx 0$, could introduce a small but systematic decrease of the average value of $\delta\mu$ and hence be the source of a systematic error.
[33]C. Domb, in *Phase Transitions and Critical Phenomena,* edited by C. Domb and M. S. Green (Academic, New York, 1974), Vol. 3, p. 357; see also J. Zinn-Justin, J. Phys. (Paris) 40, 969 (1979).
[34]K. Kawasaki, in *Phase Transitions and Critical Phenomena,* edited by C. Domb and M. S. Green (Academic, New York, 1972), Vol. 2.
[35]*Monte Carlo Methods in Statistical Physics,* edited by K. Binder (Springer, Berlin, 1979).
[36]H. Meirovitch and Z. Alexandrowicz, Mol. Phys. 34, 1027 (1977).
[37]H. Müller-Krumbhaar, Phys. Lett. A 50, 27 (1974).
[38]K. Binder, Phys. Rev. A 25, 1699 (1982).
[39]H. B. Tarko and M. E. Fisher, Phys. Rev. B 11, 1217 (1975).
[40]C. Rottman and M. Wortis, Phys. Rev. B 24, 6274 (1981); J. E. Avron, H. van Beijeren, L. S. Schulman, and R. K. P. Zia (unpublished).